PHYSICAL REVIEW B VOLUME 49, NUMBER 16 15 APRIL 1994-II

Oxides on GaAs and InAs surfaces: An x-ray-photoelectron-spectroscopy study of reference compounds and thin oxide layers

G. Hollinger, R. Skheyta-Kabbani, and M. Gendry
Laboratoire d'Electronique, LEAME, Ecole Centrale de Lyon, 69131 Ecully Cédex, France

(Received 29 November 1993)

The chemical composition of thin native oxide layers grown on GaAs and InAs by ultraviolet (UV)/ozone and thermal oxidation is investigated using x-ray-photoelectron spectroscopy. Core-level binding energies, core-level intensities, and valence-band spectra are compared with data for bulk crystalline binary or ternary As, In, and Ga oxides. The chemical compositions, which vary strongly from GaAs to InAs and from thermal to UV oxidation, appear to be controlled by both thermodynamic and kinetic factors. Only for GaAs thermal oxidation are the products predicted at thermodynamic equilibrium obtained. In all cases the native oxides can be described as single phase nonstoichiometric compounds and not as a macroscopic mixture of stoichiometric binary oxides.

I. INTRODUCTION

The oxidation of III-V semiconductors (mostly GaAs and InP) has attracted much attention in the past both for fundamental and technological reasons.[1] The nature of the interaction of oxygen with group-III and group-V elements on (110) surfaces,[2,3] the oxidation mechanism, the formation of the oxide/III-V interface, and the correlation between interface chemistry and interface electronic characteristics have been subjects of considerable interest and controversy.[4,5] III-V oxide thin films play an important role in different technological areas such as passivation,[5] preparation of wafers before epitaxy,[6,7] encapsulation, masks,[8] etc. This has motivated studies on growth processes and on the properties of these films. Oxides can be grown either by dry processes [thermal, ultraviolet (UV/ozone, and plasma oxidation] or wet processes (chemical and electrochemical oxidation). The surface and interface morphology, oxide thickness, and atomic composition can vary greatly depending on the oxidation conditions and on chemical, thermodynamic, and kinetic factors.

Surprisingly, local atomic order and chemical bonding in III-V oxides are still not well described or understood.[9] This is mainly due to the low thickness (10–100 Å) of the oxide films and to their amorphous structure. This precludes the use of x-ray and electron diffraction probes which are generally used to characterize bulk crystalline materials. Consequently, the chemical composition of such thin layers is generally evaluated using photoemission techniques [x-ray photoelectron spectroscopy (XPS) or synchrotron radiation photoemission]. From our knowledge, only one structural investigation, based on the use of reflectivity x-ray absorption spectroscopy (REXAFS), has been performed on very thin GaAs native oxide films in order to define local atomic environments around Ga and As atoms.[10]

As it is difficult to interpret core-level photoemission data unambiguously, authors very often use predictions based on the analysis of III-V-O equilibrium phase diagrams[11] to guide their interpretation (Fig. 1). As an example, GaAs oxides are very often described[1,12,13] as a mixture of stable compounds such as Ga_2O_3, As_2O_3, or As_2O_5, even if in some cases this implies the existence of Ga_2O_3-like and As_2O_3 or As_2O_5-like environments.

We have shown over the past few years that InP native oxides cannot be described only on the basis of known thermodynamically stable crystalline oxides and that InP_xO_y amorphous metastable ternary oxides with x ranging from 0.5 in UV/ozone oxides to 4.5 in anodic oxides exist in addition to the two well-known $InPO_4$ and $In(PO_3)_3$ compositions.[14–16] Such a conclusion contrasts with the mixed phase situation frequently evoked for GaAs oxides and could possibly be correlated to differences in the equilibrium phase diagrams of arsenic and phosphorus-based compounds.[11] As an example, in accordance with thermodynamics the ternary oxide $InPO_4$ is expected to result from the oxidation of InP in oxygen whereas mixtures of As_2O_3, As_2O_5, and Ga_2O_3 or In_2O_3 are expected for the oxidation of GaAs and InAs.

The aim of this work was to clarify the chemical composition of GaAs and InAs oxides and to establish whether As-based oxides are made up of nonstoichiometric ternary oxides or of a mixture of binary oxides. We used the approach defined previously in the study of InP oxides. It is based on a careful analysis of XPS core-level and valence-band spectra and on a comparison with reference

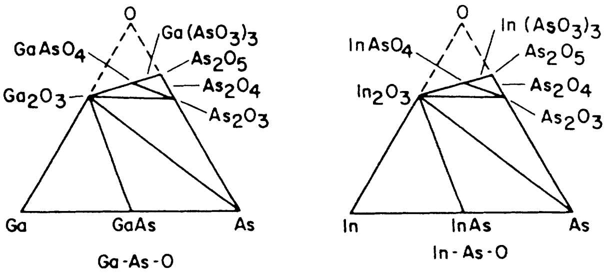

FIG. 1. Ga-As-O and In-As-O ternary condensed phase diagrams. After Ref. 11.

compound data.[14,17] To simplify, we have only considered dry oxidation processes: thermal oxidation and room temperature UV/ozone oxidation of GaAs(100) and InAs(100) surfaces in oxygen. Comparing thermal oxidation in the 350–550 °C temperature range and UV/ozone oxidation performed at room temperature is of some interest because the latter process is expected to be far from thermodynamic equilibrium whereas the former one is closer to it. Comparing GaAs oxides and InAs oxides may help to understand the oxidation mechanisms since energy reactions vary from one system to the other.

The thermal oxidation of GaAs is well documented.[1,18] At high temperature (500–700° C) polycrystalline Ga_2O_3 is the predominant product with possibly some $GaAsO_4$. At low temperature the oxidation products are amorphous phases. XPS depth profiling studies have revealed the existence of Ga_2O_3-like phases as the primary product with some elemental arsenic at the interface or within the oxide layer.[1] The UV/ozone oxidation of GaAs has been studied by McIntyre, Lau *et al.*,[19–21] and Cossu *et al.*[7] They have shown that thin oxide layers are produced which correspond to a mixture of gallium and arsenic oxides with As^{5+} and As^{3+} oxidation states.

The oxidation of InAs is much less well documented. However, Laughlin and Wilmsen[22] have reported XPS sputter-depth profiles of thermally grown oxides in the temperature range from 350 to 475 °C. In contrast to the GaAs case, a significant concentration of "As_2O_3" arsenic oxide species was found to exist. Elemental arsenic was detected, but the authors claimed that As was not entirely localized at the interface although the concentration seemed to be greater there. However, the authors did not bring any definitive evidence to support their conclusion. From our knowledge, no result exists concerning the UV/ozone oxidation of InAs.

The paper is organized as follows. In Sec. II we describe the experimental techniques. In Sec. III we present the XPS core-level and valence-band spectra for the main reference compounds of the Ga-As-O and In-As-O systems and we discuss the results in relation to known local bonding environments. In Sec. IV we discuss the chemical composition of oxides grown on InAs and GaAs by thermal oxidation and by UV/ozone oxidation.

II. EXPERIMENT

A. Sample preparation

The GaAs and InAs substrates were (100) oriented *n*-type wafers from Wacker and Sumitomo, respectively. Native oxides were removed using an HF/ethanol treatment. Thermal oxidation was performed in a quartz furnace using a constant flow of one atmosphere of oxygen, at temperatures of 350° C, 425 °C, and 460 °C, for 2 h. The films grown at 350 °C did not modify the mirror-like aspect of the substrate surfaces. GaAs oxides grown at 425–460 °C appear to be inhomogeneous with some structural defects detected by optical microscopy. A similar behavior but with fewer defects is observed for InAs.

UV/ozone oxidation was performed in an oxygen cell containing one atmosphere of oxygen in static conditions, using a low-pressure mercury lamp (Jelight model 42). Three sets of films were prepared, corresponding to 10-min, 1-h, and 3-h exposures.

The reference compounds Ga_2O_3, As_2O_3, or As_2O_5 were obtained commercially as powders. Powdered $GaAsO_4$, $InAsO_4$, and $Ga(AsO_3)_3$ were prepared using classical chemical preparation techniques.[23] Their quality was checked using x-ray diffraction.[23] Polycrystalline and monocrystalline GaAs and InAs films were prepared in a molecular-beam epitaxy (MBE) reactor attached to the XPS spectrometer. The monocrystalline epilayers were grown on (100) oriented substrates. The polycrystalline layers were prepared on the MBE sample holder (molyblock).

B. XPS analysis

The powdered reference samples were analyzed with a Hewlett-Packard (HP) 5950 A XPS spectrometer equipped with monochromatized Al $K\alpha$ radiation. Under the conditions of the experiment the Au $4f_{7/2}$ line, measured at 84.0 eV, had a full width at half maximum (FWHM) of 0.9 eV. Most of the compounds were insulators and charging effects were corrected by assuming the hydrocarbon C 1*s* peak to be at 285.2 eV.

The thin oxide films and the InAs and GaAs epitaxial and polycrystalline layers were studied in a Vacuum Science Workshop (VSW) surface analysis chamber equipped with monochromatized Al $K\alpha$ radiation. Under the conditions of the experiment the Ag $3d_{5/2}$ line, measured at 368.3 eV, had a FWHM of 0.8 eV. We measured and we discuss in this paper the In 3*d*, Ga 3*d*, O 1*s*, As 3*d*, and C 1*s* core-level spectra and the valence-band spectra for all samples. The As 2*p*, Ga 2*p*, and In 4*d* core-level spectra were also measured, but are not discussed here. In order to evaluate the in-depth homogeneity of the oxide layers, spectra were recorded at normal emission (maximum bulk sensitivity) and at a 30° takeoff angle— measured with respect to the surface— which corresponds to surface sensitive conditions.

III. REFERENCE COMPOUNDS

Three kinds of information are used to characterize a compound: (i) absolute and relative binding energies, (ii) relative core-level intensities, and (iii) shape of the valence-band spectra. Core-level and valence-band spectra were measured for a series of reference binary or ternary compounds. The valence-band spectra are shown in Fig. 2. Binding energies and energy separation, for some core levels, are presented in Table I. Due to charging effects, absolute binding energies are given with an uncertainty of ±0.3 eV. By examining this data some parameters which can help in oxide identification can be defined. The case of the In-P-O oxides was particularly favorable.[14] We were able to distinguish between In_2O_3, $InPO_4$, $In(PO_3)_3$, and P_2O_5 just from the particular shape of O 1*s* peaks. In addition $In(PO_3)_3$ and $InPO_4$ have very different valence-band shapes.

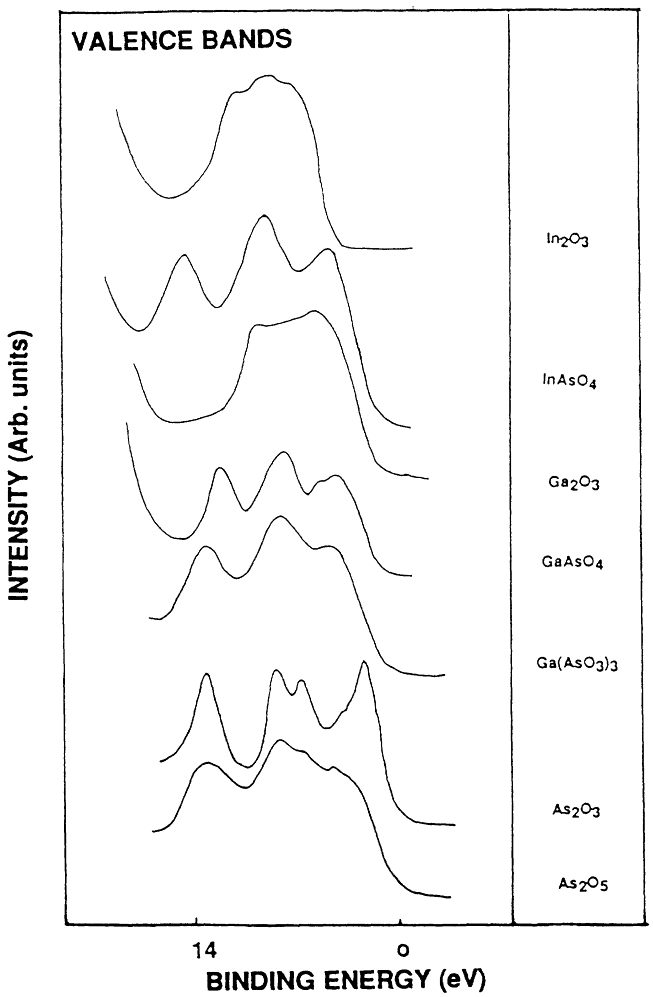

FIG. 2. XPS valence-band spectra for different bulk crystalline binary and ternary compounds of the Ga-As-O and In-As-O systems.

The case of As-based oxides appears less favorable. In order to discuss the results it is worth bearing in mind what the local atomic bonding environments in the different oxides are.[24] This information is presented in Fig. 3 and in Table II. Two points can be emphasized. (i) Like $InPO_4$, $InAsO_4$ is made up of columns of edge sharing InO_6 octahedra connected to AsO_4 tetrahedra. In contrast, $GaAsO_4$ has a tetrahedral SiO_2-like structure with GaO_4 and AsO_4 units linked through divalent oxygen atoms. (ii) In contrast to phosphates where only PO_4 units exist in P_2O_5 and $InPO_4$, a great variety of local bonding environments exist for arsenic. In addition of the ternary oxides $GaAsO_4$ and $Ga(AsO_3)_3$ (unknown structure), two stable binary oxides exist at room temperature, As_2O_3 made up of AsO_3 units and As_2O_5 made up of a combination of AsO_4 and AsO_6 units connected through divalent oxygen atoms. The latter compound could be considered as a kind of mixed valence material with the same number of "As^{4+}" and "As^{6+}" sites, giving an average As^{5+} oxidation state. This point will be discussed below.

Similarly, in β-Ga_2O_3, which is the most stable Ga_2O_3 phase, Ga atoms have two different environments. Half the atoms are in tetrahedral sites and the other half are in octahedral sites.[25]

The following comments can be expressed on the basis of the XPS data presented in Table I and in Fig. 2.

(i) Despite some broadening induced by nonuniform lateral charging of the insulating samples, O 1*s* core-level spectra always apparently have one component. This is expected for all compounds except possibly for $Ga(AsO_3)_3$ whose crystalline structure is unknown.

(ii) No splitting or broadening is detected in the As 3*d* spectra of As_2O_5, which could have been attributed to the two unequivalent As local environments. However, if some splitting exists it should be equal to or less than 0.4 eV, which means that the charge difference between the two unequivalent As atoms is small. This is in agreement with recent electronic structure calculations performed for As oxides.[25] It was found that As atoms in both tetrahedral and octahedral sites have quite similar charges, which correspond to an As^{5+} oxidation state. Notice that the large differences in bond lengths observed for AsO_6 units (≈ 1.86 Å) and AsO_4 units (≈ 1.68 Å) make As-O bonds less ionic in AsO_6 units than in AsO_4 units.

(iii) Most O 1*s* core levels have similar energies ranging between 531 and 532 eV, except for In_2O_3, which has a lower binding energy.

(iv) O 1*s*–In 3*d* and O 1*s*–Ga 3*d* energy separations

TABLE I. Binding energies (eV), energy separations, and FWHM (in parentheses) of some core levels for different reference compounds.

Compound	O 1*s*–In 3*d*	O 1*s*–Ga 3*d*	O 1*s*-As 3*d*	O 1*s*	In 3*d*	As 3*d*	Ga 3*d*
In					444.0(1.02)		
As							
InAs					444.7(0.91)	41.4(1.36)	
GaAs						41.4(1.39)	19.2(1.2)
In_2O_3	85.5			530.2(1.5)	444.7(1.49)		
Ga_2O_3		510.7		531.1(2.07)			20.4(1.73)
As_2O_3			486.5	531.9(1.43)		45.4(1.61)	
As_2O_5			485.9	532.4(1.98)		46.5(1.82)	
$InAsO_4$	85.9		485.3	531.2(2.15)	445.3(1.69)	45.9(1.92)	
$GaAsO_4$		510.6	485.4	531.9(1.86)		46.5(1.86)	21.3(1.77)
$Ga(AsO_3)_3$		511.4	486.0	532.2(2.27)		46.2(1.88)	20.8(1.55)

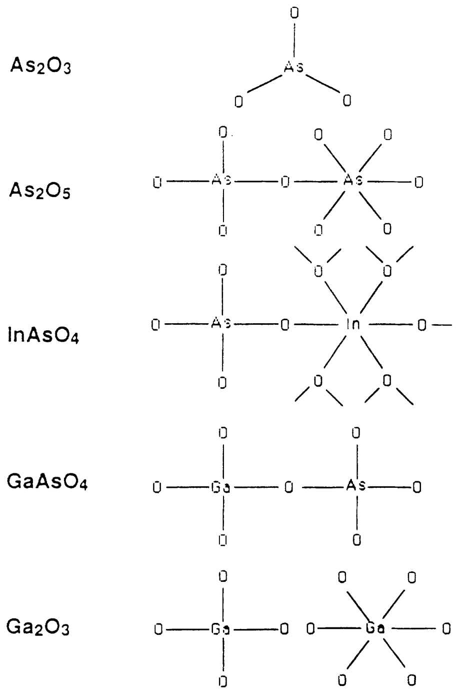

FIG. 3. Local bonding configurations in bulk crystalline binary and ternary oxides.

cannot be used to distinguish unambiguously between III-V-O ternary oxides and binary III_2O_3 oxides.

(v) The shifts observed in Ga $3d$ spectra are small. In contrast As $3d$ spectra reveal larger shifts which allow InAs or GaAs, As, As_2O_3, and As_2O_5 or $IIIAsO_4$ to be differentiated.

(vi) The O $1s$–As $3d$ energy separation is equal to 485.3 eV for $InAsO_4$ or $GaAsO_4$, 485.9 eV for As_2O_5 and 486.5 eV for As_2O_3. This should help to identify these three environments.

(vii) The valence-band shapes are very characteristic. In particular Ga_2O_3 and In_2O_3 have narrow "square" shapes. $InAsO_4$ and $GaAsO_4$ have the classical ABX_4 shape.[25,26] The As_2O_3 spectrum is characterized by four narrow structures. A characteristic feature is the presence of As $4s$ "lone pair" states at the top of the valence band.[25] In contrast, the As_2O_5 spectrum has rather broad structures. An analysis of the electronic structure of the various oxides is given in Ref. 25.

(viii) From core-level intensity measurements, sensitivity factors were established. From samples measured with the HP spectrometer we found O $1s$–As $3d=1.25$, O $1s$–In $3d=0.14$, O $1s$–Ga $3d=1.98$, As $3d$–In $3d=0.11$, and As $3d$–Ga $3d=1.6$. With the VSW spectrometer, we found As $3d$–In $3d=0.11$ and As $3d$–Ga $3d=1.2$ and we used oxygen sensitivity factors identical to those defined for the HP spectrometer.

In conclusion, although identification is more difficult than in the In-P-O case, it appears that As-based oxides can mainly be identified using atomic compositions, arsenic core-level shifts, and, to some extent, specific valence-band shapes.

IV. OXIDE LAYERS ON GaAs AND InAs

Three sets of thermal oxides and UV/ozone oxides were grown on InAs(100) and GaAs(100) surfaces. The oxidation conditions and the thicknesses of the oxide layers are reported in Table III. The samples are labeled from *a* to 1. The thicknesses of the thermal oxides were evaluated using spectroscopic ellipsometry whereas the thicknesses of the UV oxides were evaluated from the XPS core-level relative intensities of the oxide and substrate components. UV oxide thicknesses range from 10 to 30 Å. Thermal oxide thicknesses range from 30 to 300–500 Å. Oxides *a,d,e,f,g,j,k,l* are sufficiently thin to be probed entirely by XPS whereas for the thickest thermal oxides (*b,c,h,i*) the XPS data are only representative of the superficial layers. Most of the samples had a "mirrorlike" surface. Only the thick thermal oxides (*b,c,h,i*) exhibited defects on the surface. Such roughness has already been observed on GaAs by others.[27,28] It is associated to the complex oxidation mechanism of GaAs and to the departure of some arsenic atoms. In order to define the atomic composition of the oxides, the As $3d$, Ga $3d$, and In $3d$ peaks were resolved into oxide and substrate components. Only one oxide component was found in Ga and In spectra. The case of As $3d$ spectra is more complicated because several components are generally detected. In order to identify clearly the different components we numerically eliminated the 5/2 component in the As $3d_{3/2,5/2}$ spectra, assuming 0.69-eV en-

TABLE II. Coordination numbers, mean atomic distances (Å), and Gibbs free energies of formation at 298 K (Kcal/mol) for the different binary and ternary oxides (after Refs. 11, 24, and 25). The crystalline structure of $InAsO_4$ is not known.

Compound	Coordination numbers	Interatomic distances (Å) Ga-O	In-O	As-O	Gibbs energy of formation (Kcal/mol)
In_2O_3	6:4		2.27		−198.6
Ga_2O_3	4:3	1.83			−238.6
	6:4 and 3	2.00			
As_2O_3	3:2			1.79	−137.7
As_2O_5	4:2			1.69	−187
	6:2			1.81	
$InAsO_4$	6:4:2 and 3			?	−209.4
$GaAsO_4$	4:4:2	1.77		1.72	∼−223

TABLE III. Growth conditions, thicknesses (Å) for the superficial oxide layer and the interfacial As layer, and atomic compositions for different thermal and UV oxides grown on GaAs and InAs. Samples *b* and *c* are inhomogeneous laterally.

Oxidation process		Time	Temperature (°C)	Oxide thickness (Å)	Arsenic thickness (Å)	Oxide composition
				GaAs		
Thermal	*a*	2 h	350	34	6.4	$GaAs_{0.34}O_{2.8}$
	b	2 h	425		3.0	$GaAs_{0.13}O_{2.1}$
	c	2 h	460		2.9	$GaAs_{0.15}O_{2.2}$
UV	*d*	10 min	RT	8	0.3	$GaAs_{1.4}O_{3.1}$
	e	1 h	RT	17	0.9	$GaAs_{1.5}O_4$
	f	3 h	RT	27	2.0	$GaAs_{1.4}O_{4.1}$
				InAs		
Thermal	*g*	2 h	350	35	0.6	$InAs_{0.88}O_{3.3}$
	h	2 h	425	425		$InAs_{0.85}O_{3.2}$
	i	2 h	460	> 500		$InAs_{0.77}O_{3.2}$
UV	*j*	10 min	RT	10	0	$InAs_2O_8$
	k	1 h	RT	20	0	$InAs_{1.2}O_{5.1}$
	l	3 h	RT	26	2	$InAs_{1.1}O_{4.7}$

ergy separation and 0.67 spin-orbit intensity ratio. As observed in Fig. 4 and in Table IV two oxide components shifted by 3 and 4.1 eV from the substrate are always detected. They are attributed to As^{3+} and As^{5+} oxidation states, respectively. An additional 0.5–0.6-eV shifted component is often observed, essentially for GaAs oxides. This component is attributed to elemental arsenic in agreement with several authors[1,12] and not to AsO_x species as proposed by others.[3,20,21] Our results support the former explanation because the concentration of "AsO_x" should not vary strongly with oxidation conditions whereas the elemental As concentration is expected to vary from GaAs to InAs in accordance with thermodynamic considerations and should depend on oxidation conditions. This is exactly what is observed (no As for thin UV oxides on InAs). The equivalent thicknesses of the As layers were evaluated from As 3*d* core-level intensities and are reported in Table III. Angular resolved measurements showed that elemental As is located at the interface. Similarly, angular resolved measurements revealed that in both thermal and UV GaAs and InAs oxides the concentration of As^{5+} species is higher near the surface than in bulk. This was confirmed by selective chemical etching of the oxide which left As alone on the semiconductor surface.

A. Thermal oxides

In agreement with results published in the literature,[1,27,28] GaAs thermal oxides are found to be Ga rich with a composition close to Ga_2O_3. See Table III. Their valence-band spectra are similar to that of Ga_2O_3 (Fig. 6). In contrast, the InAs thermal oxides contain approximately equal to parts of As and In elements with an average composition of about $InAs_{0.8}O_{3.2}$. Their valence-band spectra have a similar shape to that of a ternary compound such as $InAsO_4$. For both GaAs and InAs oxides, As^{3+} is the dominant As component. Elemental arsenic located at the interface is detected in both cases. Only results obtained for the thin films grown at 350 °C can be interpreted significantly. A large quantity of As is found for GaAs (≈6 Å) whereas only 0.6 Å is detected for InAs. For higher growth temperatures the InAs oxide layers are thick and seem homogeneous. In contrast

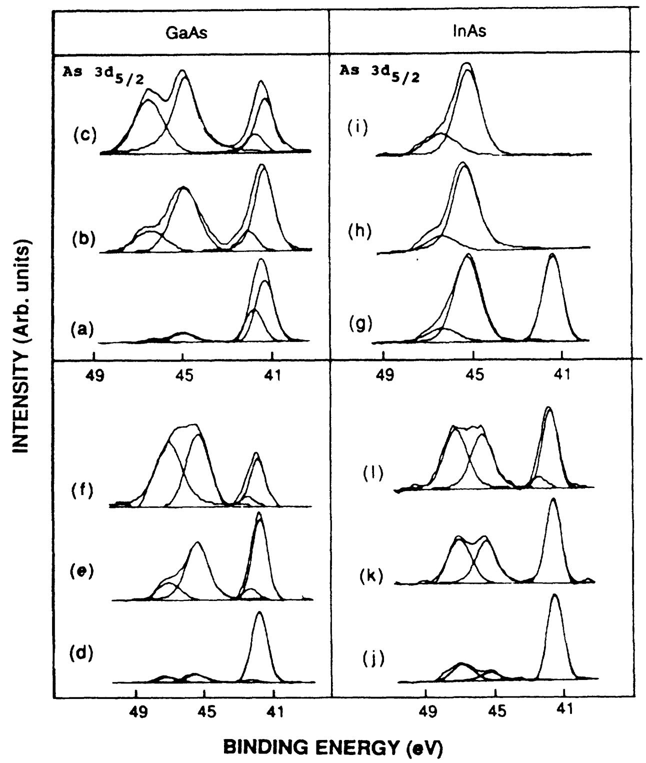

FIG. 4. As 3*d* 5/2 core-level spectra for a series of thermal and UV oxides. See text. Intensities are normalized to their maximum values. This explains why the weak components detected for high-temperature GaAs oxides [(b) and (c)] appear intense.

TABLE IV. Energy separations (eV) of some core levels, FWHM of O 1s spectra, and As^{5+}/As^{3+} core-level intensity ratio for different thermal and UV oxides grown on GaAs and InAs. Data were taken for an electron emission angle of 30° with respect to the sample surface.

Oxidation process		As^{5+} bulk	As^{3+} bulk	O 1s–As^{5+}	O1s–In 3d	O 1s–Ga 3d	O 1s FWHM	As^{5+}/As^{3+}
				GaAs				
Thermal	*a*	4.29	3.03	485.51		510.66	1.83	0.56
	b	4.32	2.91	485.30		510.61	1.66	0.41
	c	4.48	3.12	485.32		510.52	1.66	0.62
UV	*d*	4.13	2.91	485.51		510.69	2.36	1.16
	e	4.37	3.09	485.2		510.57	1.92	0.49
	f	4.24	2.93	485.4		510.69	2.01	1.02
				InAs				
Thermal	*g*	4.32	3.25	485.72	85.76		1.57	0.24
	h			485.70	85.68		1.66	0.22
	i			485.57	85.69		1.66	0.30
UV	*j*	4.24	3.05	485.72	86.07		1.48	3.01
	k	4.47	3.25	485.65	85.98		1.40	1.56
	l	4.34	3.07	485.67	85.98		1.48	1.87

the GaAs oxides are inhomogeneous which allows the detection of weak As substrate XPS components originating from defect areas. See Fig. 4.

To understand this behavior, a classical approach is to use equilibrium phase diagrams and thermodynamic predictions of interfacial reactions. We think that we can use such an approach as a guide, even if it appears that the oxide layers are made of amorphous nonstoichiometric phases and not of separate crystalline phases. The reactions can be indicative of local interfacial reactions which could lead to different microscopic products, for example, AsO_3, AsO_4, or GaO_6 units.

Three kinds of reactions could occur (11):

$$3\ O_2+2\ GaAs(InAs)\rightarrow As_2O_3+Ga_2O_3\ (In_2O_3)\ , \qquad (1)$$

$$As_2O_3+2\ GaAs(InAs)\rightarrow Ga_2O_3(In_2O_3)+4\ As\ , \qquad (2)$$

or

$$4\ O_2+2\ GaAs(InAs)\rightarrow As_2O_5+Ga_2O_3\ (In_2O_3)\ , \qquad (3)$$

$$3\ As_2O_5+10\ GaAs(InAs)\rightarrow 5\ Ga_2O_3(In_2O_3)+16\ As\ , \qquad (4)$$

or

$$2\ O_2+GaAs(InAs)\rightarrow GaAsO_4(\ InAsO_4)\ , \qquad (5)$$

$$3\ GaAsO_4(InAsO_4)+5\ GaAs(InAs)\rightarrow 4\ Ga_2O_3(In_2O_3)+8\ As\ . \qquad (6)$$

Using the terminology of Schwartz,[11] reaction (2) would be favored in weak oxidation conditions, reaction (1) in intermediate conditions, and reaction (5) in strong oxidation conditions.

The differences in the behaviors of InAs and GaAs can be interpreted as follows. Reactions of type (2) or (6) seem to be favored for GaAs since Ga_2O_3-like Ga^{3+} species and a large quantity of elemental arsenic are detected mainly. In contrast reactions of type (5) seem more favorable for InAs since ternary $InAs_xO_y$ oxides rather than In_2O_3 and As are present. This is in agreement with thermodynamic predictions which indicate that Ga_2O_3 is more stable than $GaAsO_4$ whereas $InAsO_4$ is more stable than In_2O_3, as reported in Table II.

The strongest pileup of arsenic is observed for GaAs/oxide interfaces prepared at 350 °C. It is believed that, at higher temperatures, arsenic atoms diffuse through the Ga-rich oxide layers and sublime at the surface. Some As atoms can be oxidized by the diffusing oxygen species and can lead, after reaction with "Ga_2O_3" units, to the "$GaAsO_4$"-like As^{5+} units observed in surface sensitive conditions. We note also that if some As_2O_3 or As_2O_5 phases are formed temporarily during the oxidation process, they should evaporate since these phases are volatile at temperatures higher than 350 °C. Such a mechanism should tend to leave the oxide film more Ga rich and could explain why a very rough surface is observed for thick thermal oxide films grown on GaAs and not for InAs. From the XPS data, it is clear that there are no large As_2O_3 clusters remaining for any growth conditions because no As_2O_3-like structures are detected in the XPS valence-band spectra (Fig. 6).

Thermal oxidation of InAs at 350 °C leads to oxide layers with a composition of about $InAs_{0.8}O_{3.2}$ and a very small pileup of As at the interface. The composition of surface oxides does not appear to vary strongly when the oxidation temperature increases to 425 °C and 460 °C. However, the interface composition cannot be measured due to the great thickness of the films. Since the oxides are In rich, it appears that some arsenic atoms were lost by sublimation. On the other hand, XPS core-level and valence-band data suggest that the oxide can be described as a microscopic mixture of AsO_3 and InO_6 units giving a $InAs_xO_y$ ternarylike oxide. This suggests competition between reactions (1) and (2). However, there is no evidence of phase separation since In_2O_3 and As_2O_3 are not detected. In fact, according to the oxide composition

($InAs_{0.8}O_{3.2}$) and to the shape of the As 3*d* core-level spectra, where mostly As^{3+} components are detected, it seems that the ternary oxide $InAs_xO_y$ would be closer to $InAsO_3$ than to $InAsO_4$. This could suggest that the following reaction:

$$In_2O_3+As_2O_3\rightarrow InAsO_3$$

is favored at least locally. Such a reaction could explain why As atoms remain distributed throughout the oxide film and do not sublime as happens for GaAs.

B. UV/ozone oxides

UV/ozone oxidation, performed at room temperature, produces thin oxide films on III-V semiconductor surfaces. The oxide thicknesses saturate generally at values of about 30 Å. The oxidation kinetics and the oxidation mechanisms have been discussed in detail for InP in Ref. 30. The entire oxide layers can be probed by XPS analysis. Spectra taken at normal emission and at grazing exit angles allow the detection of in-depth inhomogeneities. Results for GaAs and InAs are presented in Tables III and IV and in Figs. 4–6. The main results can be summarized as follows.

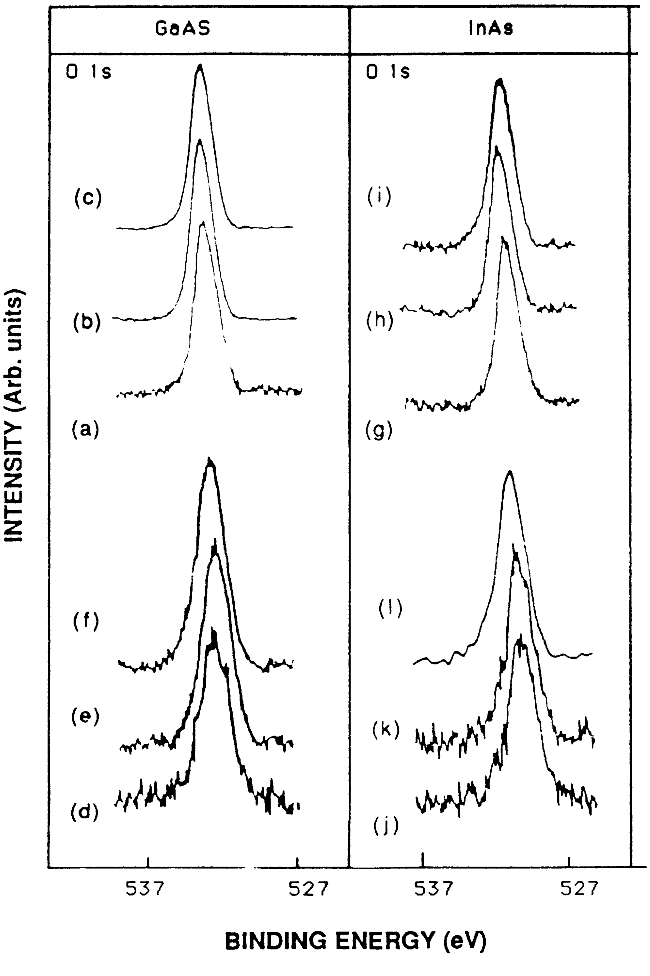

FIG. 5. O 1*s* core-level spectra for a series of thermal and UV oxides. See text.

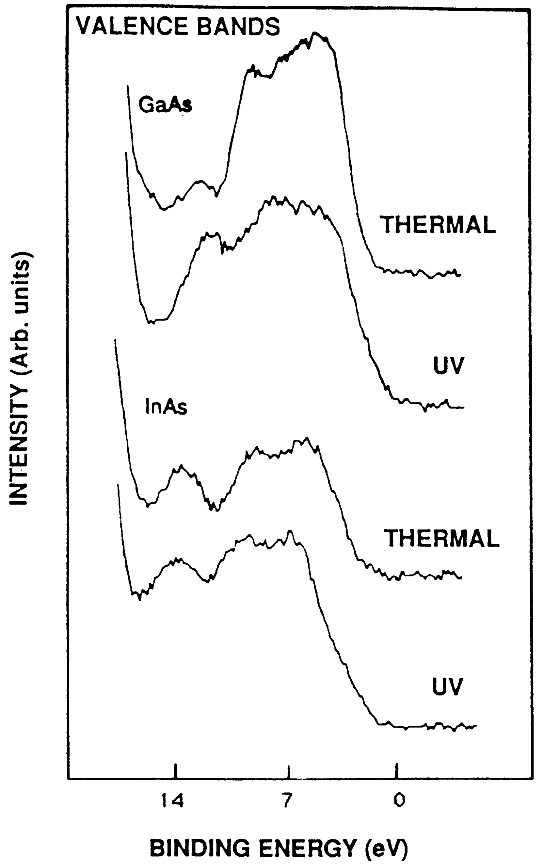

FIG. 6. Comparison of valence-band spectra for UV (3 h) and thermal (2 h at 350 °C) oxides grown on GaAs and InAs.

The same trends are observed in the compositions of both GaAs and InAs oxides which appear to be As rich. The average composition of the UV/ozone oxides are $GaAs_{1.4}O_4$ and $InAs_{1.2}O_5$, respectively. A completely different behavior was observed for UV/ozone oxides grown on InP.[16] In the latter case In-rich $InP_{0.5}O_{2.75}$ were obtained. The In/P nonstoichiometry was explained by In-P bond breaking and a departure of volatile PO_x species.[30]

The same mechanism cannot be used to explain the presence of As-rich oxides of thicknesses greater than a few monolayers. Angular resolved measurements showed that these thin UV oxide layers are rather homogeneous, but with a higher arsenic concentration at the interface than at the surface. We explain these results by speculating again about a photocarrier bond-breaking mechanism under UV irradiation. Ga-As bonds could be broken by promoting both its electrons from the valence-band bonding orbitals to the conduction-band antibonding orbitals. This phenomenon would facilitate the diffusion and the accumulation of As atoms near the III-V surface. The oxidation of such an As-rich layer would give $IIIAs_xO_y$ oxide compositions with $x>1$, as observed. Note that a similar behavior was observed for the high-temperature (550 °C) oxidation of InP,[29] where In-P bond breaking was induced by thermal effects.

As^{5+} is the dominant oxide component, in contrast to what is observed for thermal oxides. This could be related to stronger oxidizing conditions due to the action of both atomic oxygen and UV irradiation. In addition the UV oxide appear to grow far from thermodynamic equilibrium.

In accordance with thermodynamics, we expect to have ternary oxides for strong oxidation conditions [reaction (5)] and some possible interfacial reduction reactions [reaction (6)], which could produce elemental As. In fact, some elemental arsenic is detected in all cases for GaAs with increasing quantities (0.3, 0.9, and 2 Å) when the oxidation time increases from 10 min to 1 and 3 h. For InAs, no arsenic is detected after 10 min and 1 h of oxidation. Just a small quantity of arsenic is detected only after 2 h of oxidation. It is not clear whether this elemental As results directly from interfacial reactions happening during UV oxidation or is favored by the thermal annealing induced by photon irradiation (the sample temperature rises to ~60 °C).

Looking carefully at the core-level widths and core-level separations, it appears that O 1*s* core levels in GaAs UV oxides have an anomalous behavior (Table IV). A width of about 1.5–1.7 eV is found for InAs thermal and UV oxides and for GaAs thermal oxides. In contrast, GaAs UV oxides are characterized by an O 1*s* width of ~2 eV. This indicates that at least two oxygen environments exist. From Table I, it appears that O 1*s* in As_2O_5-like environments have higher binding energies than O 1*s* levels in As_2O_3, $GaAsO_4$, or Ga_2O_3. The broad O 1*s* peak measured for GaAs UV oxides could be an indication of the existence of some As_2O_5-like local bonding environments. Such a type of local order does not seem to exist in InAs UV oxides.

C. Discussion

We will now compare and discuss the differences in chemical compositions found for GaAs and InAs oxides prepared by thermal and UV oxidation. Thermal oxidation of GaAs in oxygen produces "Ga_2O_3"-rich phases and elemental arsenic at the interface, in agreement with predictions of the equilibrium phase diagram when weak oxidation conditions are assumed [reaction (2)]. A phase separation has occurred and most of the arsenic atoms have out diffused and sublimed during the oxidation process. In contrast, much less arsenic is lost during the thermal oxidation of InAs and single phase ternary "$InAsO_3$"-like oxides are produced. It appears that even if $InAsO_3$ does not exist at thermodynamic equilibrium, this compound could exist in metastable conditions at moderate oxidation temperatures.

UV oxidation of GaAs and InAs produces in both cases As-rich phases whose compositions are inconsistent with the equilibrium phase diagrams. This suggests that the oxidation mechanisms are mainly governed by photochemical effects and kinetic factors and that thermodynamics plays a minor role.

One of the main conclusions of this work is that native oxides grown on GaAs and InAs by low-temperature thermal oxidation or by room-temperature UV/ozone oxidation are generally nonstoichiometric phases (probably amorphous). Separate phases of As_2O_3, As_2O_5, and In_2O_3 do not appear to exist. However, "Ga_2O_3"-rich phases are found in GaAs thermal oxides. The AsO_3 units remaining in the films can play the same glass forming role as As_2O_3 in vitreous systems. They can interconnect Ga_2O_3 precipitates. It is worth mentioning that crystalline separate phases have only been identified unambiguously, using diffraction techniques, in thermal oxides grown at high temperature ($T > 500$ °C).

The presence of As_2O_3 or Ga_2O_3 in GaAs native oxides is often mentioned in papers based on XPS or Auger studies. However, in these papers the presence of As^{3+}, As^{5+}, and Ga^{3+} core-level peaks is wrongly correlated to As_2O_3, As_2O_5, or Ga_2O_3 phases. We think that detecting As^{3+}, As^{5+}, or Ga^{3+}-like components reveal only the presence of (i) AsO_3 units (As^{3+}), (ii) AsO_4 or AsO_6 units (As^{5+}), and (iii) GaO_4 or GaO_6 units (Ga^{3+}).

A careful analysis of the valence-band spectra indicate that these spectra cannot be described as a mixture of spectra for separate phases. Our results suggest that the oxide layers consist of single phase metastable nonstoichiometric oxides, the composition of which can vary with depth. Their structure could consist of a random microscopic mixture of pyramidal AsO_3, tetrahedral AsO_4, and octahedral AsO_6 units for As environments, tetrahedral GaO_4 or octahedral GaO_6 units for Ga environments, and InO_6 units for In environments. Oxygen atoms could exist with coordination of 2, 3, or 4. XPS data cannot help to discriminate between these possibilities and structural probes such as REXAFS would be necessary to go further in the microscopic description of these oxides.

V. CONCLUSION

This study is a step towards a better understanding of local chemical bonding in III-V native oxides. It allows the generalization of the microscopic description which is beginning to emerge on the basis of recent results obtained for InP native oxides.

Except in a few cases, we never found any evidence for the existence of stoichiometric ternary oxides or for the phase separation into binary oxides as predicted by equilibrium phase diagrams. Oxide do not generally grow close to thermodynamic equilibrium and kinetic factors very often play a major role. As III and V elements behave differently (diffusion, evaporation) a great variety of compositions can be found and the chemical composition of bulk oxide layers are generally nonuniform. However, III and V elements are always found with well-defined oxidation states which proves that thermodynamics controls the local order and the stability of the corresponding units. The ability of oxygen atoms to have coordination varying from 2 to 4 can help to build amorphous networks made up of microscopic mixtures of tetrahedral and octahedral units without structural defects. Such a picture is supported by the good electrical and passivating properties of InP native oxides.[5] The poor quality of native oxide/GaAs interfaces can be simply explained by the presence of elemental arsenic at the interface and not necessary by bonding defects in the oxide layers.

ACKNOWLEDGMENTS

We thank J. Durand for providing the $InAsO_4$, $GaAsO_4$, and $Ga(AsO_3)_3$ samples and B. Skheyta for performing the ellipsometry measurements. LEAME is URA No. 848 of CNRS.

---

[1] C. W. Wilmsen, in *Physics and Chemistry of III-V Compound Semiconductor Interfaces,* edited by C. W. Wilmsen (Plenum, New York, 1985).

[2] K. A. Bertness, J. J. Yeh, D. J. Friedman, P. H. Mahowald, A. K. Wahi, T. Kendelewicz, I. Lindau, and W. E. Spicer, Phys. Rev. B **38**, 5406 (1988).

[3] S. G. Anderson, T. Komeda, J. M. Seo, C. Capasso, G. D. Waddill, P. J. Benning, and J. H. Weaver, Phys. Rev. B **42**, 5082 (1990).

[4] H. Hasegawa and H. Ohno, J. Vac. Sci. Technol. B **4**, 1130 (1986).

[5] P. Viktorovitch, Revue Phys. Appl. **25**, 895 (1990).

[6] J. P. Contour, J. Massies, H. Fronius, and K. Ploog, Jpn. J. Appl. Phys. **27**, L167 (1988).

[7] G. Cossu, G. M. Ingo, G. Mattogno, G. Padeletti, and G. M. Proietti, Appl. Surf. Sci. **56-58**, 81 (1992).

[8] J. M. Dallesasse, N. Holonyak, Jr., A. R. Sugg, T. A. Richard, and N. El-Zein, Appl. Phys. Lett. **57**, 2844 (1990).

[9] G. Lucovsky and R. S. Bauer, J. Vac. Sci. Technol. **17**, 946 (1980).

[10] N. T. Barrett, G. N. Greaves, S. Pizzini, and K. J. Roberts, Surf. Sci. **227**, 337 (1990).

[11] G. P. Schwartz, Thin Solid Films **103**, 3 (1983).

[12] R. P. Vasquez, B. F. Lewis, and F. J. Grunthaner, Appl. Phys. Lett. **42**, 293 (1983).

[13] Z. Lu, M. T. Schmidt, R. M. Osgood, Jr., W. M. Holber, and D. V. Podlesnik, J. Vac. Sci. Technol. A **9**, 1040 (1991).

[14] G. Hollinger, E. Bergignat, J. Joseph, and Y. Robach, J. Vac. Sci. Technol. A **3**, 2082 (1985).

[15] G. Hollinger, J. Joseph, Y. Robach, E. Bergignat, B. Commere, P. Viktorovitch, and M. Froment, J. Vac. Sci. Technol. B **5**, 1108 (1987).

[16] G. Hollinger, D. Gallet, M. Gendry, M. P. Besland, and J. Joseph, Appl. Phys. Lett. **59**, 1617 (1991).

[17] G. Hollinger, C. Estrada, J. Durand, and M. Gendry, J. Microsc. Spectrosc. Electron. **13**, 31 (1988).

[18] O. R. Monteiro and J. W. Evans, J. Vac. Sci. Technol. A **7**, 49 (1989).

[19] S. Ingrey, W. M. Lau, and N. S. McIntyre, J. Vac. Sci. Technol. A **4**, 984 (1986).

[20] B. J. Flinn and N. S. McIntyre, Surf. Interface Anal. **15**, 19 (1990).

[21] W. M. Lau, R. N. S. Sodhi, and S. Ingrey, Appl. Phys. Lett. **52**, 386 (1988).

[22] D. H. Laughlin and C. W. Wilmsen, Thin Solid Films **70**, 325 (1980).

[23] J. Durand (unpublished).

[24] A. F. Wells, *Structural Inorganic Chemistry* (Clarendon, Oxford, 1984).

[25] E. A. Albanesi, S. J. Sferco, I. Lefebvre, G. Allan, and G. Hollinger, Phys. Rev. B **46**, 13 260 (1992).

[26] S. J. Sferco, G. Allan, I. Lefebvre, M. Lannoo, E. Bergignat, and G. Hollinger, Phys. Rev. B **42**, 11 042 (1990).

[27] R. Beserman, S. A. Schwarz, D. M. Hwang, and C. Y. Chen, Phys. Rev. B **44**, 3025 (1991).

[28] N. T. McDevitt and J. S. Solomon, J. Electrochem. Soc. **133**, 1913 (1986).

[29] E. Bergignat, G. Hollinger, and Y. Robach, Surf. Sci. **189/190, 353** (1987).

[30] M. P. Besland, P. Louis, Y. Robach, J. Joseph, G. Hollinger, D. Gallet, and P. Viktorovitch, Appl. Surf. Sci. **56-58**, 846 (1992).